SLAC-PUB-8041
March 1999

Measurement of the Deuteron Spin Structure Function $g_1^d(x)$ for $1\ (\mathrm{GeV}/c)^2 < Q^2 < 40\ (\mathrm{GeV}/c)^2$

The E155 Collaboration

Submitted to Physical Review Letters

Stanford Linear Accelerator Center, Stanford University, Stanford, CA 94309

Work supported by Department of Energy contract DE–AC03–76SF00515.

SLAC–PUB–8041
March 1999

Measurement of the Deuteron Spin Structure Function $g_1^d(x)$ for $1\ (\mathrm{GeV/c})^2 < Q^2 < 40\ (\mathrm{GeV/c})^2$ *

The E155 Collaboration

P.L. Anthony,[16] R.G. Arnold,[1] T. Averett,[5,*] H.R. Band,[21] M.C. Berisso,[12] H. Borel,[7] P.E. Bosted,[1] S.L. Bültmann,[19] M. Buenerd,[16,†] T. Chupp,[13] S. Churchwell,[12,‡] G.R. Court,[10] D. Crabb,[19] D. Day,[19] P. Decowski,[15] P. DePietro,[1] R. Erbacher,[16,17] R. Erickson,[16] A. Feltham,[19] H. Fonvieille,[3] E. Frlez,[19] R. Gearhart,[16] V. Ghazikhanian,[6] J. Gomez,[18] K.A. Griffioen,[20] C. Harris,[19] M.A. Houlden,[10] E.W. Hughes,[5] C.E. Hyde-Wright,[14] G. Igo,[6] S. Incerti,[3] J. Jensen,[5] J.R. Johnson,[21] P.M. King,[20] Yu.G. Kolomensky,[5,12] S.E. Kuhn,[14] R. Lindgren,[19] R.M. Lombard-Nelsen,[7] J. Marroncle,[7] J. McCarthy,[19] P. McKee,[19] W. Meyer,[4] G. Mitchell,[21] J. Mitchell,[18] M. Olson,[9,§] S. Penttila,[11] G. Peterson,[12] G.G. Petratos,[9] R. Pitthan,[16] D. Pocanic,[19] R. Prepost,[21] C. Prescott,[16] L.M. Qin,[14] B.A. Raue,[8] D. Reyna,[1] L.S. Rochester,[16] S. Rock,[1] O.A. Rondon-Aramayo,[19] F. Sabatie,[7] I. Sick,[2] T. Smith,[13] L. Sorrell,[1] F. Staley,[7] S. St.Lorant,[16] L.M. Stuart,[16,‖] Z. Szalata,[1] Y. Terrien,[7] A. Tobias,[19] L. Todor,[14] T. Toole,[1] S. Trentalange,[6] D. Walz,[16] R.C. Welsh,[13] F.R. Wesselmann,[14] T.R. Wright,[21] C.C. Young,[16] M. Zeier,[2] H. Zhu,[19] B. Zihlmann,[19]

[1]American University, Washington, D.C. 20016
[2]Institut für Physik der Universität Basel, CH-4056 Basel, Switzerland
[3]University Blaise Pascal, LPC IN2P3/CNRS F-63170 Aubiere Cedex, France
[4]Ruhr-Universität Bochum, Universitätstr. 150, Bochum, Germany
[5]California Institute of Technology, Pasadena, California 91125
[6]University of California, Los Angeles, California 90095
[7]DAPNIA-Service de Physique Nuclaire, CEA-Saclay, F-91191 Gif/Yvette Cedex, France
[8]Florida International University, Miami, Florida 33199.
[9]Kent State University, Kent, Ohio 44242
[10]University of Liverpool, Liverpool L69 3BX, United Kingdom
[11]Los Alamos National Laboratory, Los Alamos, New Mexico 87545
[12]University of Massachusetts, Amherst, Massachusetts 01003
[13]University of Michigan, Ann Arbor, Michigan 48109
[14]Old Dominion University, Norfolk, Virginia 23529
[15]Smith College, Northampton, Massachusetts 01063
[16]Stanford Linear Accelerator Center, Stanford, California 94309
[17]Stanford University, Stanford, California 94305
[18]Thomas Jefferson National Accelerator Facility, Newport News, Virginia 23606

*Work supported by Department of Energy contract DE–AC03–76SF00515.

[19]University of Virginia, Charlottesville, Virginia 22901
[20]The College of William and Mary , Williamsburg, Virginia 23187
[21]University of Wisconsin, Madison, Wisconsin 53706

Abstract

New measurements are reported on the deuteron spin structure function g_1^d. These results were obtained from deep inelastic scattering of 48.3 GeV electrons on polarized deuterons in the kinematic range $0.01 < x < 0.9$ and $1 < Q^2 < 40$ $(\mathrm{GeV/c})^2$. These are the first high dose electron scattering data obtained using lithium deuteride ($^6\mathrm{Li}^2\mathrm{H}$) as the target material. Extrapolations of the data were performed to obtain moments of g_1^d, including Γ_1^d, and the net quark polarization $\Delta\Sigma$.

PACS Numbers: 13.88.+e, 13.60.-r, 13.60.Hb, 29.25.Pj

Submitted to Physical Review Letters

Polarized deep inelastic scattering [1, 2, 3, 4, 5] is a powerful tool for studying the internal spin structure of the proton and neutron. The longitudinal spin structure function $g_1(x,Q^2)$ so obtained is sensitive to the quark spin distributions $\Delta \mathrm{q}(x,Q^2) = \mathrm{q}^{\uparrow}(x,Q^2) - q^{\downarrow}(x,Q^2)$, where the up (down) arrow refers to quark polarization parallel (anti-parallel) to the nucleon polarization. These quantities depend on x, the fractional momentum carried by the struck parton, and Q^2, the four-momentum transfer squared of the exchanged virtual photon. In this Letter, we report on new precision measurements of the deuteron spin structure function g_1^d from the SLAC E155 experiment, which ran in early 1997. These measurements, covering the range $0.01 < x < 0.9$ and $1 < Q^2 < 40$ $(\mathrm{GeV/c})^2$, are a significant improvement over previous deuteron measurements at SLAC [1]. E155 is the first high dose electron scattering experiment to use polarized $^6\mathrm{Li}^2\mathrm{H}$ (i.e. ^{6}LiD) as the deuteron target material. These data on an isoscalar target provide a particularly strong constraint on the net quark polarization, $\Delta\Sigma = \Delta u + \Delta d + \Delta s$.

The ratio of g_1 to the unpolarized structure function F_1 can be determined from measured longitudinal asymmetries $A_{\|}$ using

$$g_1/F_1 = (A_{\|}/d) + (g_2/F_1)[2Mx/(2E-\nu)], \tag{1}$$

where M is the nucleon mass, $d = (1\text{-}\epsilon)(2\text{-}y)/[y(1+\epsilon R)]$, $y = \nu/E = (E\text{-}E')/E$, $E(E')$ is the incident (scattered) electron energy, $\epsilon^{-1} = 1 + 2[1+\gamma^{-2}]\tan^2(\theta/2)$, θ is the electron scattering angle in the lab frame, $\gamma^2 = Q^2/\nu^2$, and $R(x,Q^2)$ is the ratio of longitudinal to transverse virtual photon cross sections σ_L/σ_T. The longitudinal asymmetry $A_{\|}$ is the cross section asymmetry between negative and positive helicity electron beams incident on target nucleons polarized parallel to the beam direction. In our analysis, the recent SLAC fit to R [6] and the NMC fit to F_2 [7] were used to calculate F_1. The contribution from the g_2 structure function was determined using the g_2^{WW} twist-two expression of Wandzura and Wilczek[8], given by

$$g_2^{WW}(x,Q^2) = -g_1(x,Q^2) + \int_x^1 g_1(\xi,Q^2)d\xi/\xi. \tag{2}$$

This expression was initially evaluated using the E143 fit [1] for g_1, and the process was iterated including the values for g_1 from E155. Measurements of g_2 [9] are consistent with g_2^{WW}. The transverse term in Eq. 1 is suppressed by the factor of $2Mx/(2E-\nu)$, so g_2 has only a few percent impact on the g_1 results, even if $g_2 = 0$ is used. Although emphasis was given to measurements with parallel target polarization to maximize the g_1 sensitivity, modest data samples with perpendicular target polarization were taken to measure g_2 [9].

Longitudinally polarized 48.3 GeV electron beam pulses of up to 400 ns duration were produced at 120 Hz by a circularly polarized laser beam illuminating a strained GaAs photocathode. The helicity for each pulse was selected by a 32-bit pseudo-random number generator to minimize instrumental asymmetries. The beam polarization P_b was determined periodically during the data run using Møller scattering from 20–154 μm thick Fe-Co-V polarized foils. Results from independent single arm [10] and coincidence detector systems agreed within 1%. No statistically significant deviations from the average value of $P_b = 0.813 \pm 0.020$ were seen during the experiment.

The ^{6}LiD target [11] was 3 cm long, 2.5 cm in diameter, and enclosed in an aluminum cup. Lithium deuteride [12] provides a significant improvement over the previously used deuterated ammonia, because ^{6}Li can, to first order, be treated as a polarized deuteron plus an unpolarized alpha particle, and therefore half of the nucleons in ^{6}LiD are the desired polarizable species [13]. It is also fives times as radiation resistant as $^{15}ND_3$. Pre-irradiation doses of 1.3-4.5$\times 10^{17} e^-/cm^2$ were used to create the paramagnetic centers necessary for dynamic nuclear polarization. At 1 K in a 5.004 T field, an average in-beam free deuteron polarization $\langle P_t \rangle$ of 22% was achieved using 140 GHz microwaves. The maximum value was obtained after an exposure of approximately $5\times 10^{15} e^-/cm^2$ in the 48 GeV beam. The polarization of the target material was determined by nuclear magnetic resonance measurements calibrated to the signal obtained at thermal equilibrium near 1.6 K. An overall relative uncertainty of 4% on P_t was achieved using this technique. The ^{6}Li polarization was measured to be 97% of the free deuteron polarization, consistent with predictions based on equal spin temperatures and the ratio of magnetic moments. Isotopic analysis of the target material revealed that it contained molar fractions of 0.046 for ^{7}Li and 0.024 for ^{1}H. Both of these impurities are polarizable and were accounted for in the analysis.

Scattered electrons were detected in three independent magnetic spectrometers at central angles of 2.75°, 5.5°, and 10.5° with respect to the incident beam. In the spectrometers at 2.75° and 5.5° [2], electrons were identified using two threshold gas Cherenkov counters and an electromagnetic calorimeter consisting of a 20 by 10 stack of lead glass blocks 24 radiation lengths (X_0) thick. Particle momenta and scattering angles were measured with two sets of scintillator hodoscopes. The 10.5° spectrometer was added for E155 to double the Q^2 range of the experiment. It consisted of a single dipole between two quadrupoles followed by a single scintillator hodoscope, a threshold gas Cherenkov counter, and an electromagnetic calorimeter with a preradiator (PR) section and a total absorption (TA) section. The PR section consisted of ten $2X_0$ thick lead glass bars, which were also used in the particle momentum determination, while the TA section consisted of a 5 by 6 stack of lead glass blocks $16X_0$ thick.

The experimental longitudinal ($A_\parallel$) asymmetries were determined from the numbers of scattered electrons per incident beam charge for negative (N_-) and positive (N_+) beam helicity using

$$A_\parallel^d = \left(\frac{N_- - N_+}{N_- + N_+} \frac{1}{f P_b P_t C_1} - C_2 A_\parallel^p \right) \frac{1}{f_{RC}} + A_{RC}. \tag{3}$$

The rates N_- and N_+ were corrected for contributions from charge symmetric background processes, which were measured by reversing the spectrometer polarity. This asymmetry is consistent with zero, leading to dilution corrections of 10%−15% at the lowest x bin in each spectrometer and decreasing rapidly at higher x. The rates N_- and N_+ were also corrected for mis-identified hadrons, which were typically about 2% or less of the electron candidates. Corrections for the rate dependence of the electron detection and reconstruction efficiency were a few percent for each spectrometer.

The dilution factor f is the fraction of events originating in the free deuterons. It was determined from the composition of the target materials, containers, and NMR coils in the beam, which contained 19% free deuterium, 55% ^{6}Li, 14% ^{4}He, 11% Al, and 1% N by weight.

The x dependence of the cross sections for these nuclei caused f to vary from 0.18 at low x to 0.20 at high x. The relative systematic uncertainty on f of $\sim 2\%$ was dominated by the uncertainties of the density and packing fraction of the ^{6}LiD granules.

The factors C_1 and C_2 account for the presence of several polarizable nuclear species in the target. C_1 includes the contributions from the free deuterons and ^{6}Li, and ranges from 1.77 to 1.85, with an uncertainty of ± 0.05. $C_1 f$ then gives an effective dilution factor of ~ 0.36, as compared with ~ 0.22 for $^{15}ND_3$. Calculations based on isospin conservation, shell model, solutions of Fadeev equations and a Green's function Monte Carlo provide consistent values for the valence nucleon polarization [13]. From these analyses, we conclude that the effective deuteron in ^{6}Li has a net polarization of 87% of the Li polarization. The C_2 term accounts for contributions from polarized protons in Li^{1}H and ^{7}Li. This correction is the product of the fraction of the species present in the granules and a factor for the effective polarization of the protons. The spin-3/2 ^{7}Li nucleus is described well in terms of two clusters: an α particle and a triton. The neutrons in the triton are predominantly anti-aligned, so the only significant polarized contribution comes from the proton [13]. Values for C_2 range from -0.023 to -0.030 with an uncertainty of ± 0.003. The proton asymmetry $A_{||}^p$ was obtained from a fit to world data.

Both internal [14] and external [15] radiative corrections were obtained using an iterative global fit of all data [1, 2, 3, 4, 5], including E155. Previous SLAC data were recorrected in a self-consistent manner. The radiative multiplicative factor f_{RC} and additive correction A_{RC} were determined in a manner similar to that used in E154 [2]. For x above ~ 0.3, $A_{||}$ is changed by less than 2% of its value, while at low x it is decreased by ~ -0.005. The x and Q^2 dependent systematic uncertainties on $A_{||}$ due to the radiative corrections were typically 0.001, 0.002, and 0.004 for the 2.75°, 5.5°, and 10.5° spectrometers, respectively.

The E155 results for g_1^d/F_1^d are shown in Fig. 1 as a function of Q^2. They are in good agreement with world data [1, 2, 3, 4, 5] as demonstrated by representative points from SMC and E143. These results and the g_1 values obtained from them are shown in Table 1 along with the average x and Q^2 for each bin. The data from the three spectrometers provide both large Q^2 coverage and good statistical resolution in the mid-x region. There is no significant Q^2 dependence for g_1^d/F_1^d, indicating that the polarized and unpolarized structure functions evolve similarly.

A simple parameterization was used to evolve the data to $Q^2 = 5$ (GeV/c)^2. The world data from proton, neutron, and deuteron targets [1, 2, 3, 4, 5], including E155, with $Q^2 > 1$ (GeV/c)^2 and missing mass $W > 2$ GeV were used to constrain separate proton and neutron functions of the form

$$(g_1/F_1) = x^\alpha (a + bx + cx^2)(1 + \beta/Q^2). \tag{4}$$

The deuteron data were included in the fit using the relation $g_1^d = \frac{1}{2}(g_1^p + g_1^n)(1 - 1.5\omega_D)$, where the deuteron D-state probability is $\omega_D = 0.05 \pm 0.01$. The variation [16] of ω_D with x is comparable to the uncertainty in ω_D for $x < 0.75$ and negligible compared to the statistical uncertainties for $x > 0.75$. The E155 deuteron data were included in 38 x bins to preserve shape information and ensure proper treatment of the errors. The parameters obtained from the fit for the proton (neutron) were $\alpha = 0.615$ (-0.082), $a = 0.715$ (-0.056), $b = 1.331$ (-0.319), $c = -1.766$ (0.830), and $\beta = -0.17$ (-0.14). The β values of

-0.17 ± 0.05 and -0.14 ± 0.30 are small and consistent with the data in Fig. 1. The overall fit has a χ^2 of 493 for 493 degrees of freedom.

This fit and F_1 from [6, 7] were used to evolve the measured g_1^d data to a fixed $Q_0^2 = 5$ (GeV/c)^2, shown in Fig. 2 along with xg_1^d. Integrating g_1 over the data range yields $\int_{0.01}^{0.9} g_1^d(x, Q_0^2)dx = 0.0401 \pm 0.0025(\text{stat}) \pm 0.0024(\text{syst})$. The extrapolation for the high x contribution was found to be negligible. However, the contribution from the low x region from 0 to 0.01 does not converge for Eq. 4, reinforcing the need for additional data at very low x. Using the E154 [2] and SMC [17] perturbative QCD fits for the low x extrapolation gives values of $\int_0^1 g_1^d(x, Q^2)\, dx = \Gamma_1^d = 0.0266 \pm 0.0025(\text{stat}) \pm 0.0071(\text{syst})$ and $\Gamma_1^d = 0.0291$ with comparable uncertainties, respectively.

Using the expression obtained from the operator product expansion [1], and information on the weak hyperon decay constants from [18], $\Delta\Sigma$ can be extracted from Γ_1^d. Using the E154 and SMC fits for the low x region, values of $\Delta\Sigma = 0.15 \pm 0.03 \pm 0.08$ and 0.18 (respectively) are obtained in the $\overline{MS}$ scheme. These values are well below the Ellis-Jaffe prediction of 0.58 [19], but are in agreement with previous experimental values. The precision obtained using only the E155 deuteron data is comparable with results such as the E154 NLO fit result of $0.020 \pm 0.06 \pm 0.05$ obtained using all previous world data. Improving the precision of $\Delta\Sigma$ further will require a better understanding of the very low x behavior of g_1.

The higher moments of g_1 are also of theoretical interest and are less sensitive to the extrapolation at low x. Integrating xg_1 and x^2g_1 over x at $Q_0^2 = 5$ (GeV/c)^2 yields $0.0134 \pm 0.0007(\text{stat}) \pm 0.0008(\text{syst})$ and $0.0057 \pm 0.0004(\text{stat}) \pm 0.0004(\text{syst})$ in the data region. The contributions from the low and high x regions are negligible. Lattice QCD calculations [20] predict $\int_0^1 x^2 g_1^d(x, Q^2 \sim 4\ (\text{GeV/c})^2)\ dx = 0.0064 \pm 0.0017$, which is in good agreement with $0.0061 \pm 0.0004 \pm 0.0004$ obtained by evolving the E155 data to $Q^2 = 4$ (GeV/c)^2.

Acknowledgments

We sincerely thank the SLAC Experimental Facilities group for their assistance in setting up the experiment and the SLAC Accelerator Operators group for their efficient beam delivery. This work was supported by the Department of Energy (TJNAF, Massachusetts, ODU, SLAC, Stanford, Virginia, Wisconsin, and William and Mary); the National Science Foundation (American, Kent, Michigan, and ODU); the Kent State University Research Council; the Schweizersche Nationalfonds (Basel); the Commonwealth of Virginia (Virginia); the Centre National de la Recherche Scientifique and the Commissariat a l'Energie Atomique (French groups).

References

[*] Present address: College of William and Mary, Williamsburg, Virginia 23187

[†] Permanent Address: Institut des Sciences Nucléaires, IN2P3/CNRS, 38026 Grenoble Cedex, France

[‡] Present Address: Duke University, TUNL, Durham, North Carolina 27708

[§] Present Address: St. Norbert College, De Pere, Wisconsin 54115

[|||] Present Address: Lawrence Livermore National Laboratory, Livermore, California 94551

[1] SLAC E143, K. Abe *et al.*, Phys. Rev. D **58**, 112003 (1998).

[2] SLAC E154, K. Abe *et al.*, Phys. Lett. B **405**,180 (1997); K. Abe *et al.*, Phys. Rev. Lett. **79**, 26 (1997).

[3] SMC, B. Adeva *et al.*, Phys. Rev. D **58**, 112001 (1998).

[4] HERMES, A. Airapetian *et al.*, Phys. Lett. B **442**, 484 (1998); K. Ackerstaff *et al.*, Phys. Lett. B **404**, 383 (1997).

[5] SLAC E80, M. J. Alguard *et al.*, Phys. Rev. Lett. **37**, 1261 (1976); SLAC E130, G. Baum *et al.*, Phys. Rev. Lett. **51**, 1135 (1983); SLAC E142, P. L. Anthony *et al.*, Phys. Rev. D **54**, 6620 (1996); EMC, J. Ashman *et al.*, Nucl. Phys. B **328**, 1 (1989).

[6] K. Abe *et al.*, Report No. SLAC-PUB-7927, hep-ex/9808028, accepted by Physics Letters.

[7] NMC, P. Arneodo *et al.*, Phys. Lett. B **364**, 107 (1995).

[8] S. Wandzura and F. Wilczek, Phys. Lett. B **72**, 195 (1977).

[9] P. L. Anthony *et al.*, Report No. SLAC-PUB-7983 (1998), accepted by Physics Letters, hep-ex/9901006.

[10] H. R. Band, G. Mitchell, R. Prepost, and T. Wright, Nucl. Instrum. Methods Phys. Res., Sect. A **400**, 24 (1997).

[11] D. G. Crabb and D. B. Day, Nucl. Instrum. Methods Phys. Res., Sect. A **356**, 9 (1995).

[12] S. Bültmann *et al.*, Report No. SLAC-PUB-7904 (1998), accepted by Nucl. Instrum. Methods Phys. Res., Sect. A.

[13] O. A. Rondon, Report No. aps1998dec15_002, 1998, submitted to Phys. Rev. C.

[14] T. V. Kukhto and N. M. Shumeiko, Nucl. Phys. B **219**, 412 (1983);I. V. Akusevich and N. M. Shumeiko, J. Phys. G **20**, 513 (1994).

[15] Y. S. Tsai, Report No. SLAC-PUB-848 (1971); Y. S. Tsai, Rev. Mod. Phys. **46**, 815 (1974).

[16] W. Melnitchouk, G. Piller, and A. W. Thomas, Phys. Lett. B **346**, 165 (1995).

[17] SMC, B. Adeva *et al.*, Phys. Rev. D **58**, 112002 (1998).

[18] Particle Data Group, Eur. Phys. J. C **3**, (1998).

[19] J. Ellis and R. Jaffe, Phys. Rev. D **9**, 1444 (1974); D **10**, 1669 (1974).

[20] M. Göckeler *et. al.*, Phys. Rev. D **53**, 2317 (1996).

Table 1: Results for g_1/F_1 and g_1 from this experiment with statistical (stat) and systematic uncertainties (syst).

	$\langle x \rangle$	$\langle Q^2 \rangle$	g_1/F_1 ($\pm$stat$\pm$syst)	g_1 ($\pm$stat$\pm$syst)
2.75°	0.015	1.22	-0.033 ± 0.016 ± 0.001	-0.234 ± 0.115 ± 0.011
	0.025	1.59	0.011 ± 0.014 ± 0.001	0.051 ± 0.068 ± 0.006
	0.035	2.05	0.016 ± 0.014 ± 0.001	0.059 ± 0.052 ± 0.005
	0.050	2.57	0.030 ± 0.015 ± 0.002	0.082 ± 0.041 ± 0.004
	0.080	3.24	0.059 ± 0.016 ± 0.003	0.103 ± 0.028 ± 0.005
	0.125	4.03	0.079 ± 0.021 ± 0.005	0.089 ± 0.024 ± 0.006
	0.175	4.62	0.107 ± 0.041 ± 0.008	0.083 ± 0.032 ± 0.006
	0.250	5.06	0.192 ± 0.042 ± 0.012	0.096 ± 0.021 ± 0.006
	0.350	5.51	0.301 ± 0.098 ± 0.017	0.086 ± 0.028 ± 0.005
	0.500	5.77	0.389 ± 0.129 ± 0.024	0.047 ± 0.016 ± 0.003
5.5°	0.050	4.00	-0.266 ± 0.170 ± 0.002	-0.787 ± 0.504 ± 0.006
	0.080	5.37	0.006 ± 0.020 ± 0.003	0.012 ± 0.038 ± 0.006
	0.125	7.16	0.079 ± 0.014 ± 0.005	0.094 ± 0.016 ± 0.006
	0.175	8.90	0.099 ± 0.022 ± 0.008	0.080 ± 0.018 ± 0.006
	0.250	10.62	0.184 ± 0.020 ± 0.012	0.090 ± 0.010 ± 0.006
	0.350	12.59	0.305 ± 0.044 ± 0.017	0.081 ± 0.012 ± 0.005
	0.500	14.01	0.349 ± 0.057 ± 0.025	0.034 ± 0.006 ± 0.002
	0.750	15.73	0.576 ± 0.220 ± 0.029	0.006 ± 0.002 ± 0.001
10.5°	0.125	10.98	-0.020 ± 0.095 ± 0.006	-0.025 ± 0.117 ± 0.008
	0.175	13.19	0.157 ± 0.042 ± 0.008	0.127 ± 0.034 ± 0.007
	0.250	17.22	0.194 ± 0.027 ± 0.012	0.094 ± 0.013 ± 0.006
	0.350	22.65	0.309 ± 0.053 ± 0.017	0.077 ± 0.013 ± 0.005
	0.500	26.97	0.330 ± 0.092 ± 0.024	0.028 ± 0.008 ± 0.002
	0.750	34.79	0.428 ± 0.903 ± 0.028	0.003 ± 0.007 ± 0.001

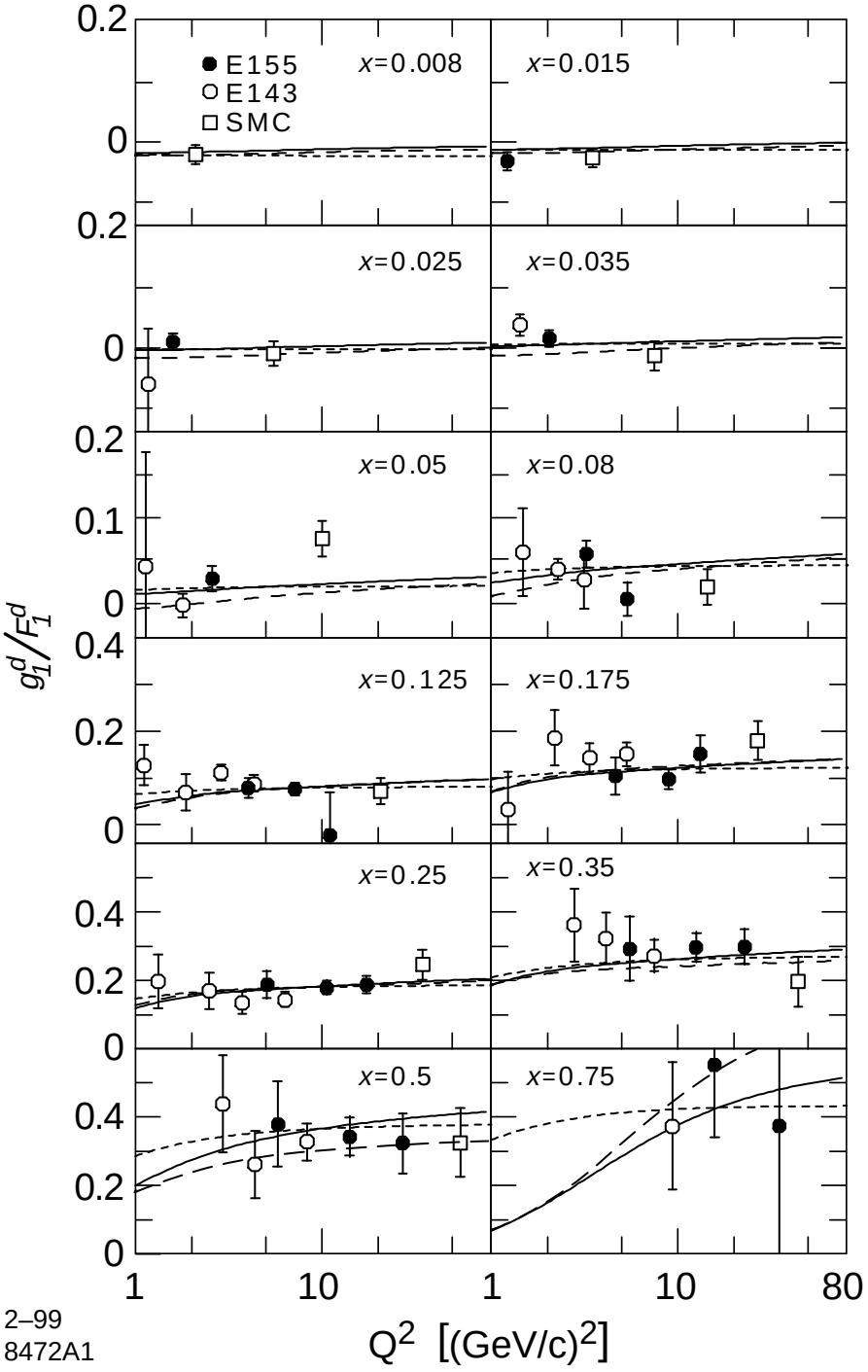

Figure 1: Values of g_1^d/F_1^d vs. Q^2 at various values of x for this experiment (filled circles), E143 (open circles), and SMC (open boxes). The inner bars are statistical uncertainties, while the outer bars include systematic errors added in quadrature. The curves are our parameterized fit (short-dashed), the E154 NLO fit [2] (solid), and the SMC NLO fit (long-dashed) [17].

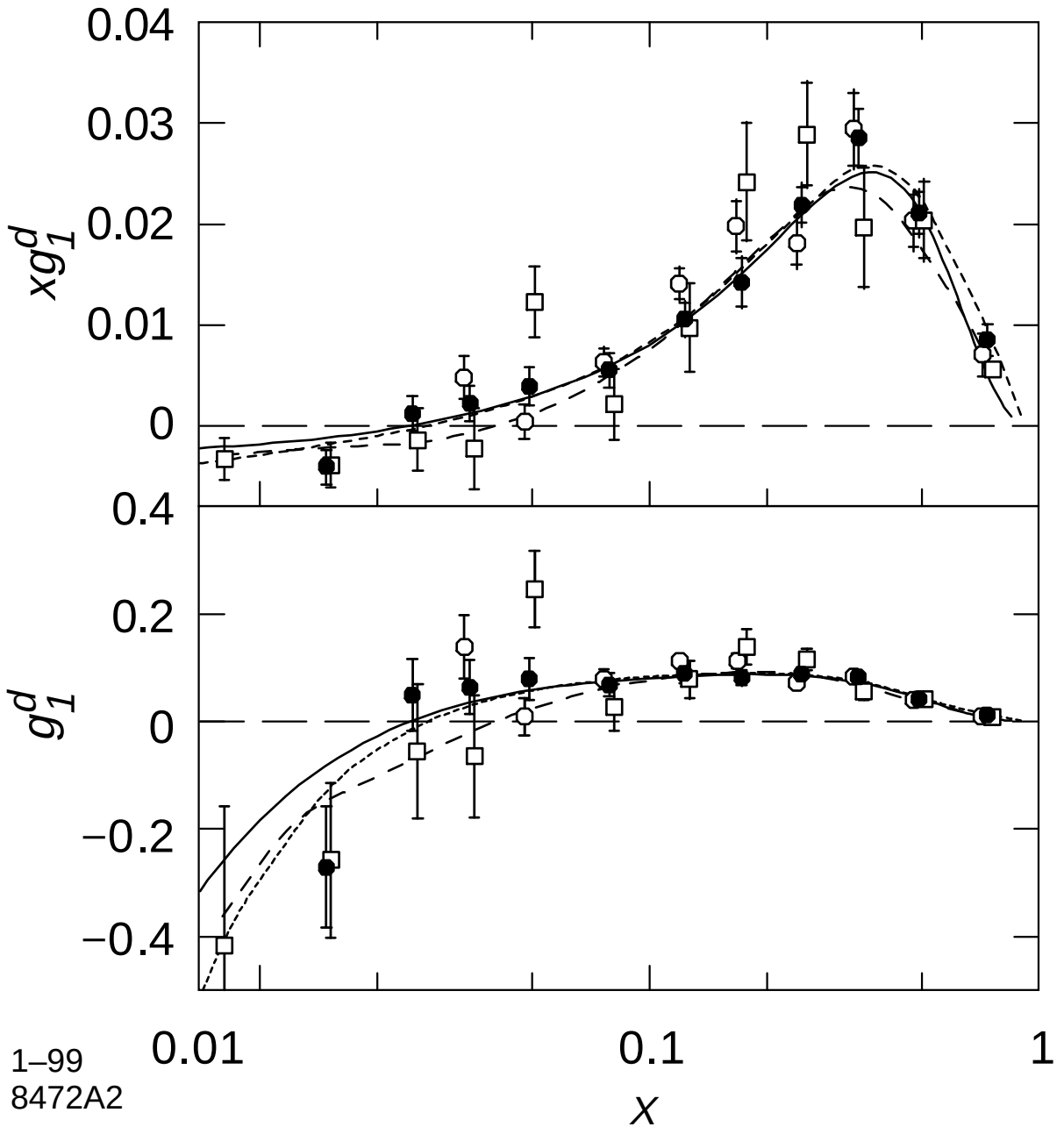

Figure 2: Values of xg_1^d (a) and g_1^d (b) evolved to Q^2 of 5 $(GeV/c)^2$ using Eq. 4. The symbols and curves are as in Fig. 1.